

Ligand field effect tuned magnetic behaviors of two chain compounds based on $\text{Mn}^{\text{III}}_3\text{O}$ units: from slow magnetic relaxation to metamagnetism[†]

Yue-Ling Bai,^{*a} Xiaoli Bao,^a Shourong Zhu,^a Jianhui Fang^a and Jun Tao^{*b}

^aDepartment of Chemistry, College of Sciences, Shanghai University, Shanghai 200444, P. R. China,

^bDepartment of Chemistry, State Key Laboratory for Physical Chemistry of Solid Surfaces, Xiamen

University, Xiamen 361005, People's Republic of China

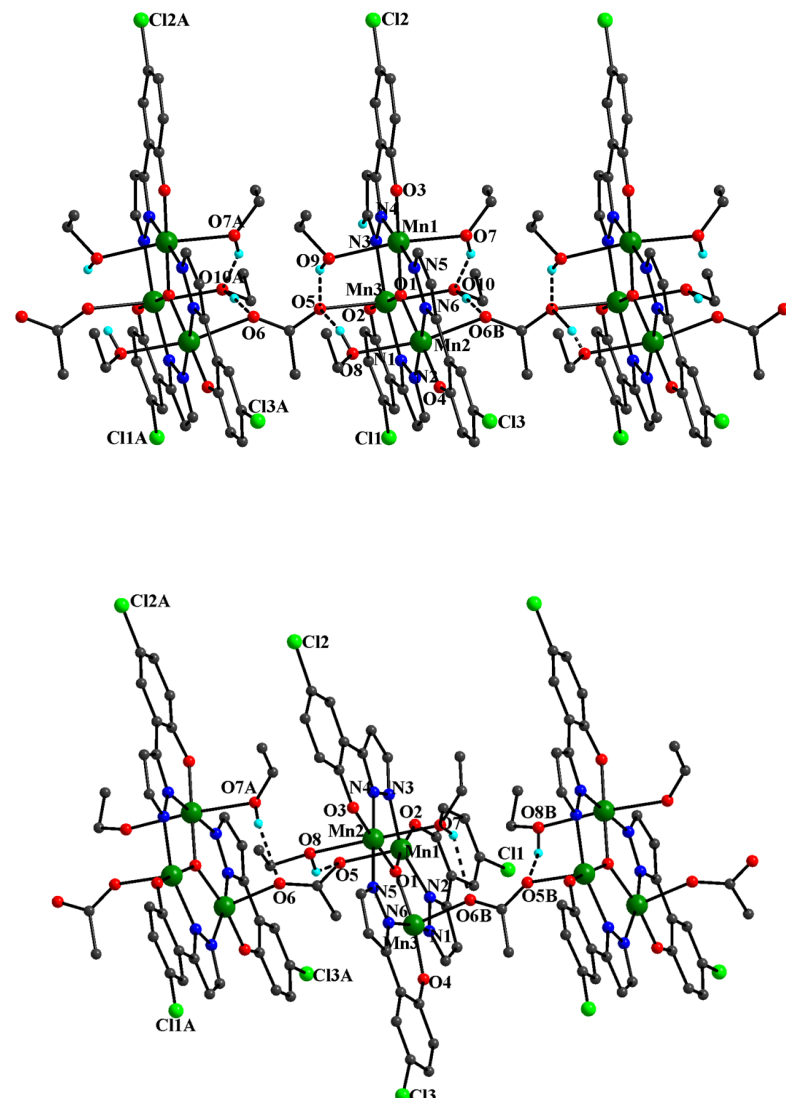


Figure S1. 1D chain structures of **1** (top) and **2** (bottom) with the intrachain hydrogen bonds.

Table S1. Hydrogen-Bond Distances (\AA) for Complexes **1** and **2**.

1				2	
O7–H \cdots O10	3.174(9)	O10–H \cdots O6	2.923(7)	O7–H \cdots O6	2.790(5)
O8–H \cdots O5	3.095(8)	O9–H \cdots O5	2.728(7)	O8–H \cdots O5	2.830(5)

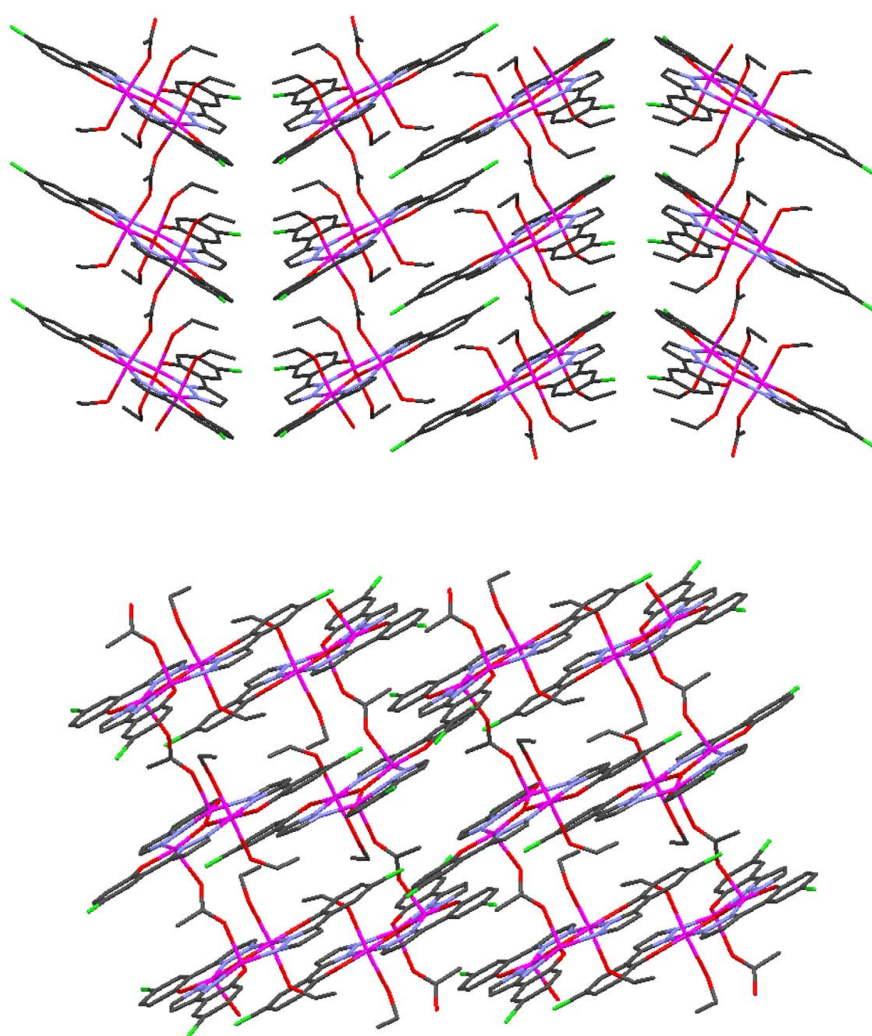


Figure S2. Two-dimensional stacking modes of **1** (top) and **2** (bottom).

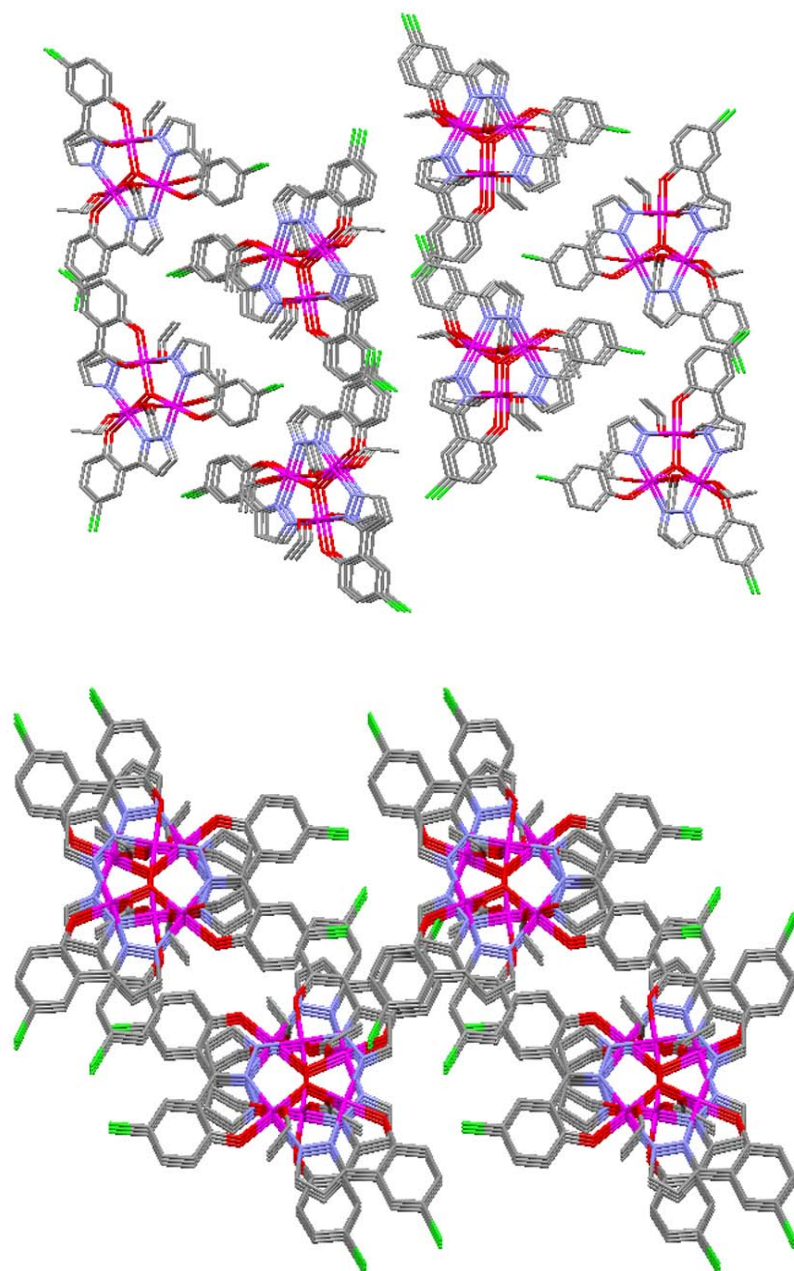


Figure S3. Three-dimensional supramolecular structures viewed down the a axis of **1** (top) and down the c axis of **2**, which showing Mn···Cl short contacts and π - π weak interactions between the adjacent chains (bottom).

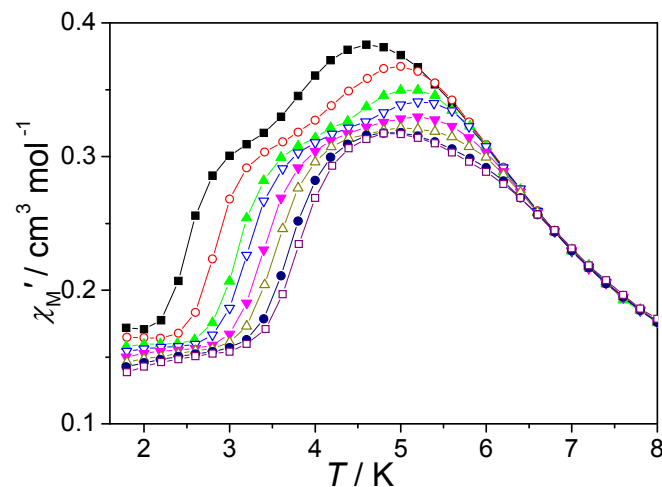


Figure S4. Temperature dependence of χ_M'' for **1** at zero dc field and a ac field of 3 Oe.

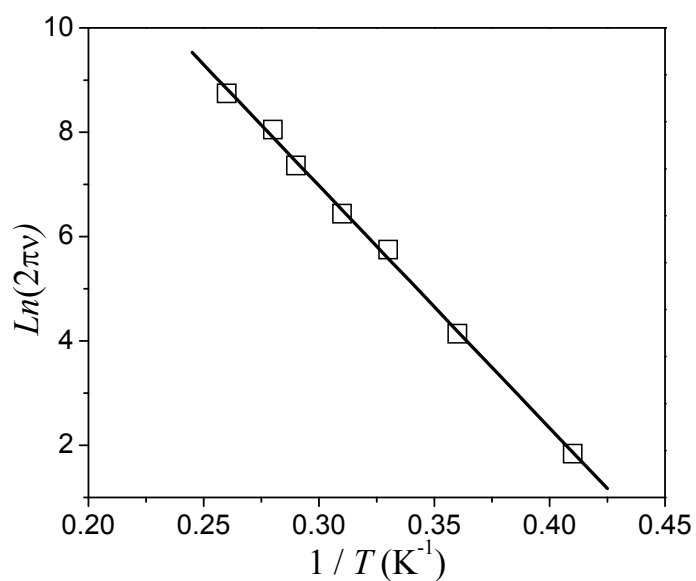


Figure S5. Arrhenius plot using AC data. The line is the fit of the thermally activated region to the Arrhenius equation.

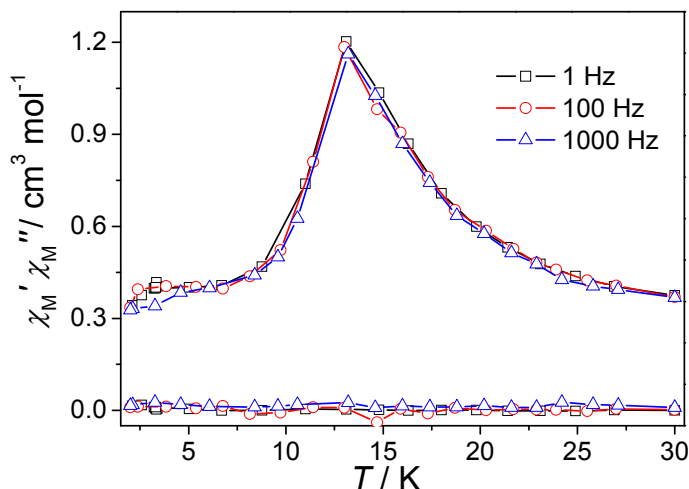


Figure S6. Temperature-dependent χ_M' and χ_M'' in the frequency range of 1-1000 Hz for **2**.

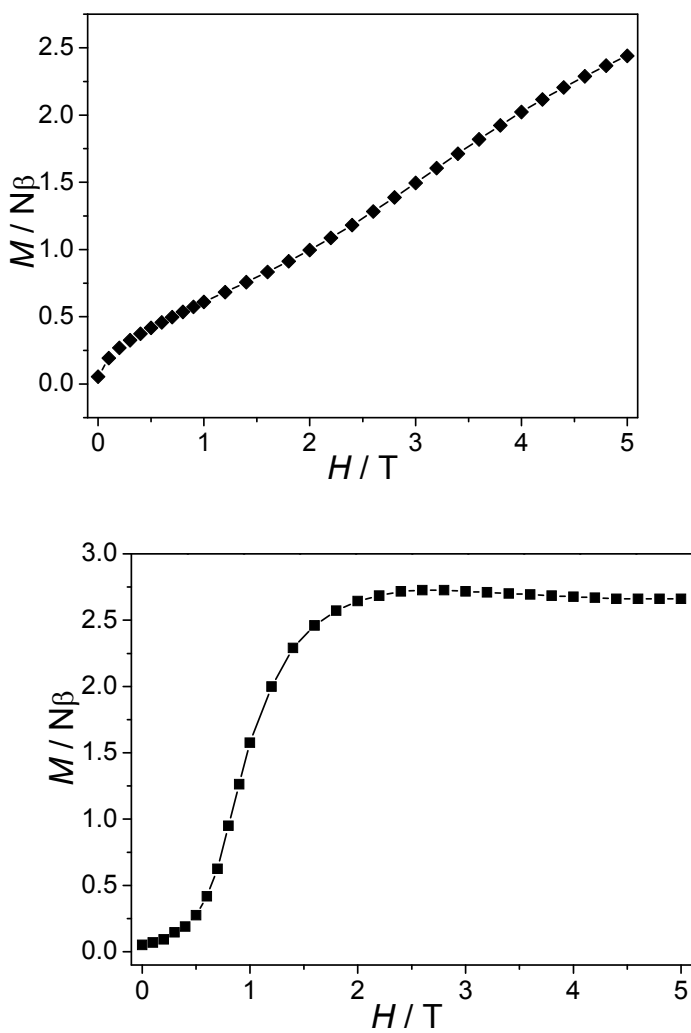


Figure S7. Field-dependent magnetization of **1** (top) and **2** (bottom).

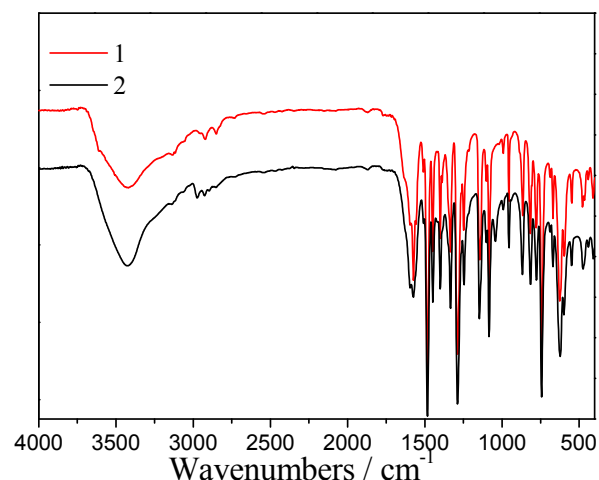


Figure S8. Infrared spectra of complexes **1** and **2**.

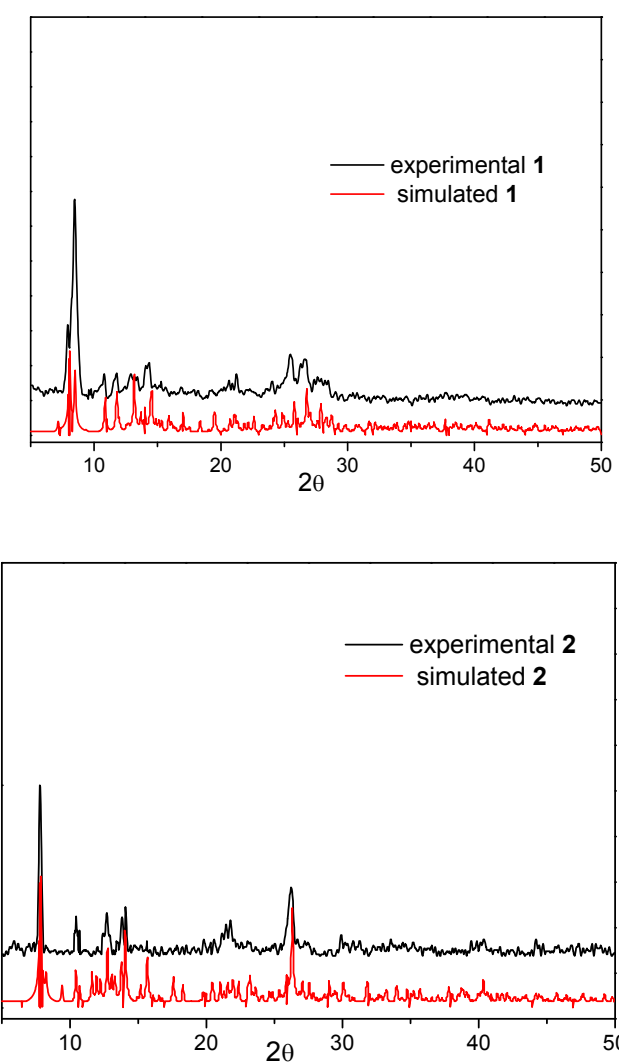


Figure S8. The XRPD diffraction patterns of complexes **1** and **2**.